Permeability reduction in porous materials by in situ formed silica gel

Permeability reduction in porous materials by *in situ* formed silica gel

H. J. Castelijns
Department of Geotechnology, Delft University of Technology, P.O. Box 5048, 2600 GA Delft, The Netherlands and Department of Applied Physics, Eindhoven University of Technology, P.O. Box 513, 5600 MB Eindhoven, The Netherlands

G. W. Scherer
Department of Civil and Environmental Engineering, Princeton Institute for the Science and Technology of Materials, Princeton University, Princeton, New Jersey 08544, USA

L. Pel
Department of Applied Physics, Eindhoven University of Technology, P.O. Box 513, 5600 MB Eindhoven, The Netherlands

P. L. J. Zitha[a)]
Department of Geotechnology, Delft University of Technology, P.O. Box 5048, 2600 GA Delft, The Netherlands

(Received 14 February 2007; accepted 30 September 2007; published online 3 December 2007)

The effect of *in situ* formed silica gel on the permeability of a porous material was investigated experimentally. Gelling solutions of tetra-methyl-ortho-silicate (TMOS) and methanol in water were imbibed into dry sandstone plates and cured for several days. The permeability of the untreated sandstone is on the order of 1 μm^2, whereas the intrinsic permeability of the silica alcogel is 5–6 orders of magnitude lower. The method of beam bending was employed to measure concurrently the permeability D and Young's modulus E_p of cylindrical gel rods, prepared from the TMOS-based sol-gel solutions. Second, the permeabilities and moduli of the treated sandstones were measured. For both types of samples the gel structure was varied by varying the concentration of the TMOS in a solution and the pH of the water used. The parameters D and E_p follow from a detailed analysis of the measured relaxation of the load that is applied to the sample under constant deflection. In case of the gels, the relaxation was interpreted using common expressions for hydrodynamic relaxation and viscoelastic (VE) relaxation. It was found that the permeability of the gels decreases with increasing silica content and that acid-catalyzed gels exhibit a significantly lower permeability than base-catalyzed gels. The modulus E_p increases with increasing silica content and aging time. The relaxation data of the sandstone—treated with gel—exhibited a more complex behavior. The normalized load curves showed hydrodynamic relaxation as well as strong and fast VE relaxation. The relaxation data for the rock samples treated with the lowest concentration gel was fitted successfully with the predictions. For higher concentrations the fit was less accurate, but the permeability estimates were within an order of magnitude. The overall permeability of the treated rock is higher than the intrinsic permeability of the gels; this indicates that the gel does not completely fill the pore space. Nevertheless, the permeability is reduced by a factor 10^4 with respect to untreated sandstone, and therefore the gel adequately blocks the pores. © *2007 American Institute of Physics*. [DOI: 10.1063/1.2817577]

I. INTRODUCTION

The permeability of porous materials can be reduced by introducing polymer solutions or gel-forming chemicals in the pore space. This effect is found in numerous applications in the oil industry[1,2] and in subsurface waste containment.[3] Silica gels can be readily formed according to the sol-gel principle[4,5] by the hydrolysis of a suitable alkoxy-silane precursor, e.g., tetra-methyl-ortho-silicate (TMOS) or $Si(OCH_3)_4$, and the subsequent condensation of its reaction product, i.e., silanol (Si-OH) groups. The gel time of the sol-gel solution and the mechanical properties of the resulting gel depend strongly on temperature, pH, type, and concentration of the catalyst, and the initial concentration of the precursor.[4] An interesting aspect of this type of chemical is that the alkoxy silane can be mixed with most hydrocarbons and thereby introduced in a porous material under a two-phase flow condition. In such a case the compound transfers from the oleic to the aqueous phase and reacts with the water to produce a silica gel. Recently, the mechanisms of this process in various two-phase model systems were studied using a nuclear magnetic resonance (NMR) technique.[6]

The method of beam bending[7,8] was employed to measure the permeability of TMOS-based silica gels and to measure the permeability of a porous material treated with gel that was formed *in situ* under single phase conditions. Gelling solutions of TMOS, methanol, and water were imbibed in dried sandstone plates and allowed to react and cure. Gel rods were made from the sol-gel solutions in order to com-

a)Author to whom correspondence should be addressed. Electronic mail: p.l.j.zitha@tudelft.nl

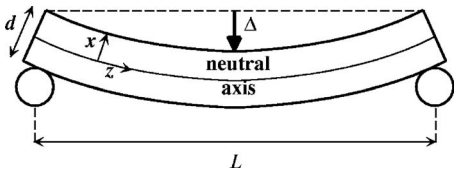

FIG. 1. Schematic of a three-point beam bending. The deflection Δ is sustained with a force *W*. The diameter of the cylindrical beam is *d*, and the distance between the supports is *L*.

pare the intrinsic permeability of the gel with the permeability of the treated rock. In the beam bending method a saturated porous material, immersed in a liquid bath, is subject to a three-point bending. Upon bending of the sample a hydrodynamic pressure gradient builds up and the pore liquid flows until the pressure is equilibrated. A constant deflection is imposed on the sample and the load (force) required to maintain that deflection is measured. The load relaxes with a typical decay time from which the permeability can be derived. The beam bending technique is especially adequate for low-permeability materials such as silica gels,[7] porous glass,[9] or cement paste.[10] In addition, the beam bending method concurrently yields the elastic moduli and the degree of viscoelasticity (if any), both of which are of interest with respect to the mechanical properties and performance of the gels and rock samples. As such, beam bending constitutes an alternative method to determine elastic moduli and fluid relaxation properties of saturated porous materials next to, for example, (laboratory) seismic methods[11,12] or axial compression methods.[13] The purpose of this work is to investigate whether the gel effectively fills the pore space and whether the reduction of the overall permeability is sensitive to parameters such as *p*H and TMOS concentration.

II. THEORETICAL BACKGROUND

For a cylinder with diameter *d* made of an elastic porous material, the load *W* needed to sustain a constant deflection Δ (see Fig. 1) is given by[14]

$$\frac{W(t)}{W(0)} = R(t) = 1 - A + A\sum_{n=1}^{\infty} \frac{8}{\beta_n^2} \exp\left(-\frac{\beta_n^2 t}{\tau_R}\right), \tag{1}$$

where A is the amount of hydrodynamic relaxation, β_n's are the roots of the Bessel functions $J_1(\beta_n)=0$, and τ_R is the hydrodynamic relaxation time. In the case of a gel, the solid material comprising the porous body is usually very compliant such that compressibility effects in the system can be omitted. The amount of hydrodynamic relaxation A is then simply a function of the Poisson ratio ν_p, that is, $A=(1-2\nu_p)/3$. The hydrodynamic relaxation time τ_R is given by[9]

$$\tau_R = \frac{(1-2\nu_p)\eta_L d^2}{4DG_p}, \tag{2}$$

where η_L is the pore liquid viscosity, D is the permeability, and G_p is the shear modulus of the (drained) porous system. The latter follows from Young's modulus E_p through the relation $E_p=2(1+\nu_p)G_p$. Young's modulus is derived from the initial load $W(0)$ and the moment of inertia, $I=\pi d^4/64$, using the following equation:

$$E_p = \frac{W(0)(1-A)L^3}{48\Delta I}, \tag{3}$$

where L is the span in the three-point bending experiment.

For a rectangular isotropic beam (plate) of elastic porous material, with thickness $2a$ and width $2b$, the normalized load as a function of the reduced time $\theta=t/\tau_R$ is given by[15]

$$\frac{W(\theta)}{W(0)} = R(\theta) = 1 - A + AS_1(\theta)S_2(\kappa\theta), \tag{4}$$

where $\kappa=a^2/b^2$ and the functions S_1 and S_2 are given approximately by[16]

$$S_1(\theta) \approx \exp\left[-\left(\frac{6}{\sqrt{\pi}}\right)\left(\frac{\theta^{0.5}-\theta^{2.5}}{1-\theta^{0.551}}\right)\right], \tag{5}$$

$$S_2(\theta) \approx \exp\left[-\left(\frac{2}{\sqrt{\pi}}\right)\left(\frac{\theta^{0.5}-\theta^{2.094}}{1-\theta^{0.670}}\right)\right]. \tag{6}$$

Due to the high modulus of the rock, the compressibility effects have to be taken into account. The parameter A is then replaced by[10]

$$A = \frac{\left(\frac{1-2\nu_p}{3}\right)\left(1-\frac{K_p}{K_S}\right)^2}{1-\frac{K_p}{K_S}+(1-\rho)\left(\frac{K_p}{K_L}-\frac{K_p}{K_S}\right)}, \tag{7}$$

in which K_p is the bulk modulus of the drained network, K_S is the bulk modulus of the solid constituting the porous network, K_L is the bulk modulus of the pore fluid, and ρ is the volume fraction of the solid content. The hydrodynamic relaxation time τ_R is related to the permeability D and the viscosity of the pore fluid η_L by[10]

$$\tau_R = \left\{\frac{2(1+\nu_p)}{3K_p} + \frac{1-\rho}{K_L} + \frac{1}{K_S}\left[\rho - \frac{4(1+\nu_p)}{3} - \left(\frac{1-2\nu_p}{3}\right) \times \left(\frac{K_p}{K_S}\right)\right]\right\}\left(\frac{\eta_L a^2}{D}\right). \tag{8}$$

The bulk modulus K_L is known for most common liquids, and the bulk modulus K_p equals $E_p/3(1-2\nu_p)$. The approximation $K_p/K_S \approx \rho^2$ can be used to estimate K_S.[10]

Many materials, including aged gels that still contain a certain amount of water, show viscoelastic (VE) behavior. When the characteristic time of viscoelastic relaxation is at least an order of magnitude longer than the characteristic time of hydrodynamic relaxation, the total load relaxation $W(t)/W(0)$ is adequately represented by the product of the hydrodynamic relaxation function $R(t)$, as described above, and an uniaxial stress relaxation function, Ψ_{VE}:[17]

$$\frac{W(t)}{W(0)} = R(t)\Psi_{\mathrm{VE}}(t). \tag{9}$$

The function Ψ_{VE} is essentially an empirical function and can be inferred from experimental data. However, for many systems the VE relaxation can be adequately described by a stretched exponential

$$\Psi_{VE} = \exp\left[-\left(\frac{t}{\tau_{VE}}\right)^{\alpha}\right], \tag{10}$$

where τ_{VE} is the VE relaxation time and α is a parameter $(0 \leq \alpha \leq 1)$.

III. EXPERIMENTAL SECTION

A. Materials

The Bentheim sandstone was obtained from a Bad-Bentheim quarry in Germany. Rectangular plates were sawed from a single block. The length and the width of the plates were 160 ± 5 mm and 25.2 ± 0.4 mm, respectively. The thickness of the plates varied between 8.05 and 10.10 mm. For each plate the thickness and width were checked at several positions on the plate surface. The precision of the thickness and width was about 0.05 mm. The sawed plates were dried at 60 °C for 5 days.

Bentheim is a quasihomogeneous sandstone without distinct bedding planes or other forms of anisotropy. Mercury intrusion porosimetry (MIP) on a same batch of Bentheim sandstone indicated that the rock has a narrow pore size distribution with an average pore size of 33 ± 10 μm and a total porosity of about 0.22. The permeability of the rock with respect to water, which was measured on several cylindrical cores using a custom-made core injection setup, was found to be 1.6 ± 0.3 μm^2. Bentheim sandstone is quartz rich with little clay content. To test the presence of clays small rock slabs were soaked in water and their length was monitored in a dynamic mechanical analyzer (DMA, type Perkin Elmer DMA 7e). In addition, the rock was analyzed in a scanning electron microscope (SEM, type FEI XL30 FEG-SEM) equipped for energy-dispersive x-ray spectroscopy (EDX, type PGT-IMIX PTS EDX). A fractured surface was coated with gold. The coating is needed to prevent the accumulation of static electric fields at the sample during imaging due to the electron irradiation. Another piece of rock was ground and analyzed using x-ray diffraction (XRD) in a Rigaku Miniflex apparatus.

The TMOS was obtained from Acros Organics (99% pure). De-ionized water was used for the hydrolysis reaction. The homogenization chemical used was methanol (Fisher Scientific, 99.9% pure). Ethanol (Pharmco, dehydrated, 200 Proof) was used to exchange with the mother liquid of the gels after curing. For the beam bending measurements on the rock samples the pore liquid was exchanged with glycerol (Acros Organics, 99+% pure).

Buffer solutions of the water were made by dissolving the following chemicals. The acid solution (pH=3.1) contained 8.47 g of citric acid, 3.22 g of NaOH, and 2.18 g of HCl per liter. The alkaline solution (pH=9.25) contained 0.1M of ammonium-hydroxide and 5.12 g/l of ammonium-chloride (about 0.1M). The latter was diluted with de-ionized water (with a ratio of 1:9) to yield a second alkaline solution with a pH of 8.8.

B. Preparation of gels and rock samples

The sol-gel solutions were prepared by first mixing TMOS with methanol in various ratios to form homogeneous mixtures. The water (acid or alkaline) was added gradually to each mixture. The water/TMOS molar ratio was always equal to 4:1. The corresponding total volume fraction of TMOS in solution varied between 0.35 and 0.55. The solutions were homogenized by stirring during 1 min. The solutions were cast in cylindrical Teflon molds with an inner diameter of 11.5 ± 0.1 mm and a length of about 13 cm. After several days of curing at room temperature the gel rods were removed from the molds and immersed in ethanol with an excess volume of about 10 to 1 for at least 1 day, after which the gels were put into a second bath of fresh ethanol for several days. This procedure was applied to maximize the exchange of the mother liquid in the gels with ethanol, so that the viscosity of the pore liquid is known, and in order to minimize further aging of the gels and minimize the degree of viscoelasticity. Scherer showed that when the pore liquid is exchanged, using various alcohols, the measurement of the permeability of a gel yields consistent results.[7,18] The gel time of the sol-gel solutions was not systematically measured. However, the occurrence of gelation of each solution was verified by casting part of each solution in transparent vessels and checking the ability of the solution to flow 24 h after preparation. All solutions gelled within 24 h. The solutions prepared using the pH=9.25 buffer gelled relatively fast within minutes or hours depending on the TMOS concentration, and much faster compared to the solutions prepared with the diluted buffer (pH=8.8). In the remainder of this work the degree of aging of the gels refers to combined curing and aging time of the gels with respect to the instant the solutions were prepared.

Gelling solutions that were prepared as described above for the gel rods were imbibed into the dry rock samples followed by complete immersion in the solution for 10 s. The imbibition, driven by capillary rise, was initiated by slowly lowering the sandstone plates into the solution, such that the shortest dimension of the plates was directed vertically. The saturation of a sandstone plate was indicated by a color change of the sandstone surface as the solution imbibed, and was completed within 10 s. Subsequently, the rock samples were tightly wrapped in several layers of aluminum foil. Plastic foil was wound around the aluminum. This way the evaporation of the gelling solution or drying of the resulting gel near the rock surface was minimized and the aluminum could easily be removed from the treated rock samples. Similar exchange procedures used for the gels were applied to the rock samples. First, the rock samples were immersed in pure ethanol for an extended period to arrest the curing. Next, the samples were put into a mixture of ethanol and glycerol (50 vol %) to exchange part of the ethanol in the pores with glycerol. Finally, the samples were immersed in glycerol for several days in order to maximize the exchange of the pore liquid with glycerol. With respect to the overall pore volume of the rock samples the excess volume of the glycerol was about 25 to 1. The use of a high-viscosity liquid such as glycerol was necessary in order to prevent the hydrodynamic relaxation from being too fast with respect to the temporal resolution and accuracy of the beam bending method, since the rock samples have high moduli on the order of 10 GPa.

TABLE I. The properties of the gel rods and beam bending results. ϕ_{Si} is the estimated volume fraction of silica assuming full hydrolysis and condensation, and corrected for the volume contraction of the gel. The *p*H listed is the *p*H of the water used in the hydrolysis reaction. The parameter C_S represents the amount of sodium-chloride (NaCl) added to the gelling solution.

Series	ϕ_{Si}	*p*H	C_S (mM)	Aging time	E_p (MPa)	D (nm^2)
I	0.113±0.007	3.1	0	43 h	5.9±0.2	1.04±0.06
	0.131±0.008	3.1	0	43 h	12.2±0.5	0.67±0.03
	0.149±0.009	3.1	0	43 h	22.8±0.9	0.38±0.02
II	0.123±0.007	3.1	0	91 h	18.6±0.7	0.66±0.03
	0.123±0.007	3.1	40	91 h	15.9±0.6	0.72±0.04
	0.123±0.007	3.1	60	91 h	15.1±0.6	0.76±0.05
	0.123±0.007	3.1	80	91 h	15.5±0.6	0.72±0.04
III	0.098±0.005	9.25	0	72 h	6.9±0.3	14.8±0.7
	0.098±0.005	9.25	40	72 h	7.3±0.3	18.2±0.8
	0.098±0.005	9.25	60	72 h	7.0±0.3	26±2
IV	0.078±0.004	8.8	0	72 h	1.4±0.1	40±2
	0.092±0.005	8.8	0	72 h	2.9±0.1	28±2
	0.100±0.005	8.8	0	72 h	4.0±0.2	20±1

C. Beam bending setup

An extensive description of the beam bending apparatus was given in a previous publication.[9] Two equivalent setups were used, both of which were situated in an incubator. The first setup was used for the gel measurements, which were done at room temperature. The temperature was stable during each run with fluctuations smaller than 1 °C. The second setup was used for the sandstone measurements. The temperature was controlled to 26±0.5 °C. Each setup contains a stainless steel bath that was filled with ethanol for the gel measurements and glycerol for the sandstone measurements. The gel samples were aligned at a fixed position using V-notch supports consisting of 6.35 mm diam rollers set at an angle of 90° with respect to each other, and forming 45° angles with the horizontal plane. The pushrod, comprising an iron core and stainless steel hammerhead end, was mounted onto the load cell. The load cell (SENSOTEC), with a capacity of ±50 g, was mounted onto the stepper motor (UltraMotion). The displacement of the pushrod was monitored through a linear-variable differential transformer (LVDT, Macrosensors). The span (L) of the supports was 110 mm.

The sandstone plates were supported by two different stainless steel supports. One consisted of a recessed ball, and the other of a pivoting cylinder. This configuration was chosen to prevent torsion. The span in this case was 150 mm. A round-tipped pushrod (diameter=6.3 mm) was used to bend the plates. A load cell with a capacity of ±1000 g was mounted onto the stepper motor. In addition, a 1000 g counter weight was mounted on the pushrod.

The rock samples and gel rods were put in the bath at least 30 min in advance of the bending experiment in order to equilibrate thermally and mechanically. During bending deflections of about 1 or 1.5 mm were applied to the gels, whereas a deflection of about 35 μm was applied to the rock samples. The small deflection for the rock samples was chosen because of the limited load capacity of the system and in order to prevent the rock samples from cracking or breaking. Due to the small deflection with respect to the surface roughness—the grain size of the sandstone is on the order of 50–500 μm—the bending measurement is sensitive to the effect of slipping of the pushrod at the surface or slipping of the rock on the supports. Test measurements indicated that this effect occurred by yielding unrealistically low moduli (E_p) for some samples and scattered results when a sample was repeatedly measured. Therefore, the samples were preloaded with a net load of about 100 g prior to the equilibration period to promote a more stable settling of the rock and pushrod. The total load upon deflection is on the order of 1 kg.

The maximum strain in the samples was about 6×10^{-3} in case of the gels, and about 9×10^{-5} in case of the sandstone beams. The strains are well within the linear range, and therefore the relaxation times are not dependent on the bending amplitude.

IV. RESULTS AND DISCUSSION

A. Gels

1. Gel properties

Four series of gel rods were prepared. The TMOS concentration was varied in series I and IV. The concentration was kept fixed in series II and III, however, extra salt, in the form of sodium-chloride (NaCl), was added in various concentrations, C_S, up to 80 mM. The effect of additional salt on the gel properties was investigated in consideration of an application of the gel in natural reservoirs, since the water found in most reservoirs is saline. The properties of the gel rods are listed in Table I. The parameter ϕ_{Si} is a measure for the total silica content of the alcogels based on the initial TMOS content and on the assumption that hydrolysis and

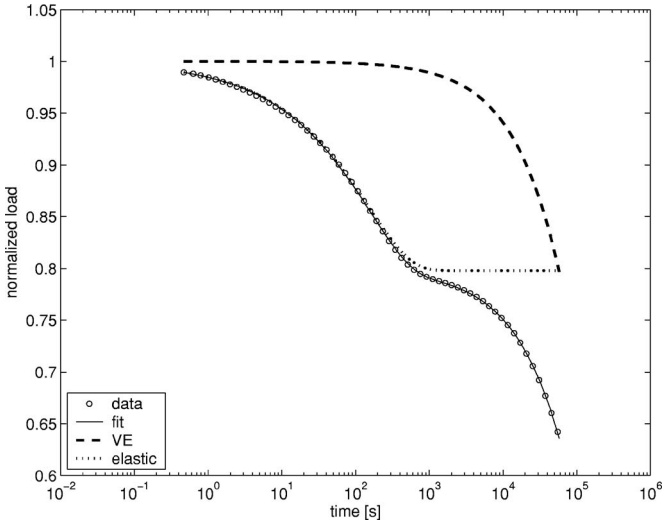

FIG. 2. Results of the beam bending experiment on gel rod (ϕ_{Si} $=0.123\pm0.007$, pH$=3.1$, no extra salt, aging time 91 h). The total fit is the product of hydrodynamic relaxation (dotted line) and viscoelastic (VE) relaxation (dashed line). The number density of the data points of the normalized load, indicated by the circles, is reduced to one-fourth for the sake of clarity.

condensation are complete. However, complete condensation implies the silica network would condense into nonporous quartz, which is not the case. Neither does the estimate account for possible washing out of polysiloxane molecules in the exchange process. Still, this measure is used to indicate the silica content of the gels. The values for ϕ_{Si} were corrected for volume contraction effects due to syneresis. Especially, the gels prepared with the acid solution (pH$=3.1$) showed a significant degree of radial contraction after aging. Because the gels are prone to breaking or cracking when exposed to air or any physical contact, the dimensions were not checked rigorously. Instead, the diameter was measured for one or two rods per series. The diameter of the acid-catalyzed gels was found to be 10.40 ± 0.10 mm after aging, whereas the diameter of the molds was 11.5 ± 0.1 mm. The dimensions were measured with a digital caliper having an accuracy of ±10 μm. The diameter of the base-catalyzed gels reduced to 11.20 ± 0.10 mm (pH$=9.25$) and 11.15 ± 0.10 mm (pH$=8.8$), respectively. The higher degree of shrinkage for the low pH gels compared to the high pH gels was also observed by Hdach *et al.*[19] for similar gels. Although the length of the gel rods could not be checked, due to the type of molds used, it is assumed that the shrinkage occurred uniformly in all three dimensions. The volume contraction factor is therefore equal to $(d_{final}/d_{initial})^3$.

2. Relaxation analysis

The data obtained from the beam bending measurements was analyzed in terms of the applied load versus time. The normalized load of each measurement was plotted and fitted with Eq. (9) using the hydrodynamic relaxation expression for cylinders [Eq. (1)] and the stretched exponential function [Eq. (10)] for the viscoelastic contribution. The measured relaxation and the fit were in excellent agreement for each gel rod. Figure 2 shows the results for one of the gel rods ($\phi_{Si}=0.123\pm0.007$, pH$=3.1$, no extra salt added, aging time 91 h). It can be observed in Fig. 2 that the gel exhibits a significant degree of VE relaxation, but the effect is only important on a time scale much longer than the time scale of the hydrodynamic relaxation, and both relaxation effects are well separated. Similar VE behavior was exhibited by all other gel rods. The VE relaxation is attributed to the presence of water in the pores, and the chemical attack of the water on the present siloxane bonds in the network.[7,20] Therefore, the exchange of the mother liquid with ethanol appears to be incomplete; nevertheless, the hydrodynamic relaxation could readily be extracted from the relaxation data.

For the gels the fit yields the following parameters. First, Poisson's ratio ν_p was directly calculated from the amount of hydrodynamic relaxation A resulting from the fit. The average ν_p was found to be 0.20 ± 0.02. The modulus E_p follows from A and the initial load W_0. The bulk shear modulus G_p is subsequently derived from E_p using Poisson's ratio. The fit also yields τ_R from which the permeability D is calculated using Eq. (2). The viscosity η_L of ethanol is about 1.07 mPa s at room temperature.[21] The measured moduli and permeabilities for the gel rods are listed in Table I and are further discussed below.

3. Acid-catalyzed gels

In series I (pH$=3.1$, total reaction and aging time of 43 h, and with varying ϕ_{Si}) the modulus E_p increases from 5.9 ± 0.2 MPa for the lowest (approximate) silica fraction, $\phi_{Si}=0.113\pm0.007$, to 22.8 ± 0.9 MPa for the highest fraction, $\phi_{Si}=0.149\pm0.009$. The gels of series II were cured and aged for 91 h and contain a varying amount of additional sodium-chloride. The modulus of the first gel with $C_S=0$ is 18.6 ± 0.7 MPa, which is high compared to the moduli of the gels in series I. Due to aging, the silica network becomes more consolidated, leading to enhanced elastic moduli. The addition of sodium-chloride to the gelling solution resulted in lower values of E_p of about 15.5 MPa but with no clear correlation to C_S within the range considered. According to Martin and Odinek,[22] the presence of small amounts of salt has little influence on the structure and growth of acid-catalyzed silica alcogels. The little variation of E_p for series II is in agreement with this finding, though the difference in E_p between the gel without extra salt (E_p is about 20% higher) and the gels with extra salt cannot be explained at this point.

The permeability D of the acid-catalyzed gels is on the order of 1 nm^2. In series I the permeability decreases from 1.04 ± 0.06 nm^2 for the lowest silica fraction to 0.38 ± 0.02 nm^2 for the highest fraction. The average permeability of the gels in series II is 0.72 ± 0.04 nm^2, which corresponds well with the permeability results of series I given the silica fractions ϕ_{Si}. The additional salt slightly increases the permeability, but this is not a clear function of concentration.

4. Base-catalyzed gels

In series IV (pH$=8.8$, total reaction and aging time of 72 h, and varying ϕ_{Si}) the modulus E_p increases from

1.4±0.1 MPa for the lowest silica fraction, $\phi_{Si}=0.078\pm0.004$, to 4.0±0.2 MPa for the highest fraction, $\phi_{Si}=0.100\pm0.005$. The moduli of the gels in series III (pH =9.25) have an average value of 7.1±0.3 MPa and appear to be independent of C_S within the range considered. The average modulus is high with respect to the moduli of the gels in the other series given the approximate silica densities ϕ_{Si}. The faster gelation of the sol-gel solutions in series III compared to the gels in series IV implies that the effective aging time was longer for the gels in series III, so that higher values for E_p are expected. In general, the modulus E_p for the acid and base-catalyzed gels is a strong function of ϕ_{Si}, and there is no significant difference in the order of magnitude of E_p for both types of gels given the different values of ϕ_{Si}.

For the gels in series III the permeability increases from 14.8±0.7 nm^2 for $C_S=0$ mM to 26±2 for $C_S=60$ mM. Although the additional sodium-chloride did not affect E_p, the permeability is strongly affected when C_S increases from 0 to 60 mM. The permeability of the gels in series IV decreases from 40±2 nm^2 for the lowest silica fraction to 20±1 nm^2 for the highest silica fraction.

The base-catalyzed gels exhibit permeabilities 10–100 times greater in magnitude than the permeabilities of the acid-catalyzed gel, which cannot be explained by the difference in the approximate silica fraction. The higher permeability for the base-catalyzed gel is due to the different pore structure, i.e., during the sol-gel reaction the silica forms thicker branches and larger aggregates than in acid systems, resulting in bigger pores at a given total silica concentration. The permeability of silica gels can be estimated using a Carman–Kozeny type of equation, such as[9,23]

$$D=\frac{(1-\phi_{Si})r_w^2}{4\kappa_w(\phi_{Si})}, \tag{11}$$

where r_w is the mean pore radius of the gel and κ_w is the Kozeny constant. The latter can be approximated by[9]

$$\kappa_w(\phi)\approx 1.0+6.05\phi^{0.5}-8.60\phi+6.56\phi^{1.5}. \tag{12}$$

Given the solid fractions of the gels, κ_w varies between 2.16 and 2.43. The experimental values of D against ϕ_{Si} for series I and IV can adequately be fitted with Eq. (11), yielding $r_w=53\pm5$ nm for the base-catalyzed gels and $r_w=8.9\pm0.4$ nm for the acid-catalyzed gels.

B. Sandstone beams

1. Beam bending of untreated sandstone

The response of a few untreated sandstone beams upon bending was checked in order to determine the moduli and the degree of VE behavior. The first measurement consisted of a dynamic Young modulus test on a dry rock sample. An oscillating deflection, in the form of a sawtooth, was imposed on the sample with a frequency of 0.05 Hz and an amplitude of 10 μm, yielding $E_p=11.3\pm0.2$ GPa. Subsequently, the rock sample was saturated with acid water (pH =3.1) and E_p dropped to 7.6±0.1 GPa. Repeated measurements, performed over 6 days, yielded the same constant value of 7.5±0.1 GPa.

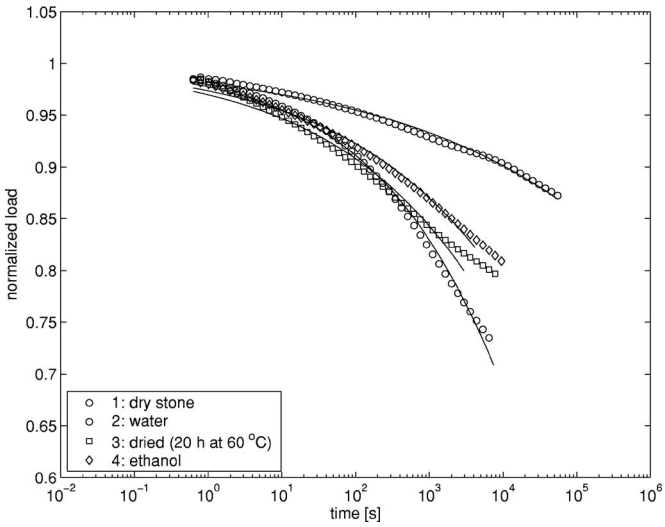

FIG. 3. Relaxation of a normalized load on untreated sandstone in a beam bending experiment. The condition of the sandstone is indicated in the legend. The absolute load varied among the different cycles. The solid lines indicate the fits with a stretched exponential.

A second dry, untreated rock sample was subjected to a constant deflection of about 35 μm, during which the load was measured. The normalized load curve is shown in Fig. 3. The modulus of the dry rock sample is $E_p=11.2\pm0.2$ GPa. The normalized load gradually relaxed to about 0.87 within 17 h. Next, the rock sample was saturated with demineralized water. Again, a bending experiment was conducted yielding a reduced modulus, i.e., $E_p=6.9\pm0.1$ GPa, and a higher degree of relaxation (see Fig. 3). Since the hydrodynamic relaxation, due to the flow of water in the gel-free pores, occurs within several microseconds, the observed relaxation is due to VE effects, similar to the case with the dry rock. Subsequently, the rock sample was dried again at 60 °C for 20 h and a third cycle under dry conditions was performed. The modulus was partly restored, having a value of 9.7±0.2 GPa. The degree of VE relaxation remained similar to that of the wet case. Finally, the bath was filled with ethanol and a fourth bending test was conducted. The modulus decreased to 9.2±0.1 GPa. The degree of VE relaxation was comparable to that of the third cycle (see Fig. 3). The relaxation curves were fitted to the stretched exponential function (see Fig. 3). Table II contains the resulting fit parameters. A decreasing τ_{VE} and increasing α imply an increasing degree of VE relaxation within a fixed time interval.

Similar VE behavior was observed in beam bending experiments on other types of sandstone by Jiménez González and Scherer.[24] The sandstones used were rich in clay and

TABLE II. The results of fit on normalized load for untreated sandstone sample using a stretched exponential. The modulus E_p is derived from the initial load.

Cycle	Condition	τ_{VE} (10^6 s)	α	E_p (GPa)
1	Dry	3700±400	0.177±0.001	11.2±0.2
2	Water-saturated	0.25±0.01	0.304±0.002	6.9±0.1
3	Redried (20 h at 60 °C)	1.3±0.1	0.248±0.003	9.7±0.2
4	Ethanol-saturated	4.0±0.3	0.238±0.002	9.2±0.1

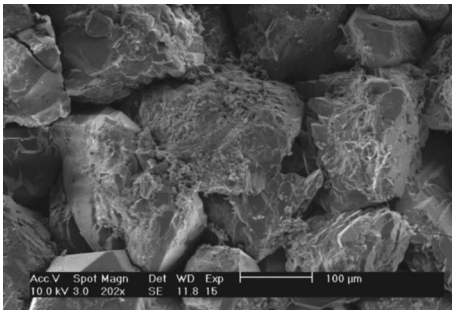

FIG. 4. Scanning electron microscope image of Bentheim sandstone.

exhibited swelling behavior as they were saturated with water. The dilatometry tests on the Bentheim sandstone showed no change in length upon wetting the samples, thus the presence of swelling clays is negligible. A significant reduction (up to 20%) of the Young modulus of sandstone by the presence of water was also found by Mann and Fatt[13] for other types of sandstone. Further, the Young modulus of Bentheim sandstone is lower compared to less permeable sandstone (as determined by other methods[13,25]).

2. SEM and XRD analysis on untreated sandstone

Several surface features were imaged and analyzed for chemical composition. A SEM image of the surface obtained at a low magnification is given in Fig. 4. The image clearly shows the coarse structure of the grains, which are held together by siliceous cement. Although the SEM-EDX analysis is semiquantitative at best, a little amount of clay was found in local spots on the sample surface. The clay mainly consisted of silica and aluminum without other cations, and is likely in the form of kaolinite. Contamination of the nonswelling clay due to cations introduced by the buffered solutions in the treated sandstone may enhance the swelling behavior. The XRD results only showed quartz, which indicates that the clay found in the SEM analysis was only present in small quantities. Despite the absence of swelling clays the grains appear to slip when a load is applied on the rock sample. The presence of water significantly reduces the elastic modulus of the rock and leads to an enhanced degree of VE relaxation with respect to a dry rock sample.

3. Beam bending of treated sandstone

The experimental results obtained for two series of treated sandstone are discussed in this section. The rock samples in series A were treated with acid-catalyzed gel whereas the rock samples in series B were treated with base-catalyzed gel. The TMOS concentration was varied in both series, but no additional sodium-chloride was added to the gelling solutions. The properties of the treated rock samples are listed in Table III. The total reaction and aging time was 72 h for all rock samples. Glycerol from fresh and tightly sealed bottles was used in the bath and for the exchange with the original pore liquid. Exposure to air was avoided as much as possible for the glycerol in the exchange bath. Therefore, it is assumed that the glycerol in the samples is free of water so that the viscosity at 26 °C is ±0.870 Pa s.[26] The bulk modulus K_L is 4.80 GPa.[26] The normalized load curves for series A and B are shown in Figs. 5 and 6, respectively. The total measurement time for each curve is about 1 h. Two experiments in series A were extended to more than 10 h. All load curves show a monotonic decrease within the times of measurement, and none of the load curves reach a plateau. The overall degree of decrease in magnitude of the normalized load appears to be scattered and increasing with the estimated ϕ_{Si}. The total amount of hydrodynamic relaxation A, which is independent of the permeability, can be approximated using Eq. (7). Poisson's ratio is unknown, but we used $\nu_p=0.25$, which is a good estimate for sedimentary rocks.[27] The elastic modulus E_p is about 10 GPa, so that $K_p=6.7$ GPa. The solid fraction is $\rho\approx 0.8$, and therefore $K_S\approx 10.5$ GPa. Calculation of A then yields a value of 0.04.

Using the estimated maximum of A and the measured initial load values, the moduli of the treated samples were determined. The results are listed in Table III. The samples in series A have an average modulus of 10±1 GPa. Three of the samples in series B show a higher modulus of about 15 GPa, whereas the other two have a modulus of about 11 GPa.

TABLE III. The properties of the treated sandstone samples. ϕ_{Si} is the estimated volume fraction of silica assuming full hydrolysis and condensation, without correction for shrinkage. The thickness of the plates is given by $2a$. The superscript b is used to indicate the duplicate samples prepared with the same gelling solutions as the complementary samples.

Series	ϕ_{Si}	pH	$2a$ (±0.05 mm)	E_p (GPa)	D (nm^2)	A[-]
A	0.071	3.1	10.00	9.3±0.3	59±7	0.049±0.002
	0.071^b	3.1	9.80	8.5±0.1	95±13	0.047±0.001
	0.084	3.1	8.92	11.3±0.5	112±15	0.110±0.004
	0.084^b	3.1	8.05	10.1±0.1	20±2	0.097±0.002
	0.097	3.1	9.40	11.6±0.2	8±1	0.166±0.005
	0.097^b	3.1	9.70	10.6±0.2	91±12	0.160±0.005
B	0.071	8.8	10.00	14.8±0.1	94±9	0.044±0.001
	0.071^b	8.8	9.70	14.4±0.1	56±5	0.042±0.001
	0.084	8.8	9.42	15.4±0.2	52±4	0.071±0.001
	0.097	8.8	8.90	10.7±0.3	14±1	0.226±0.002
	0.097^b	8.8	10.10	11.1±0.2	50±4	0.153±0.003

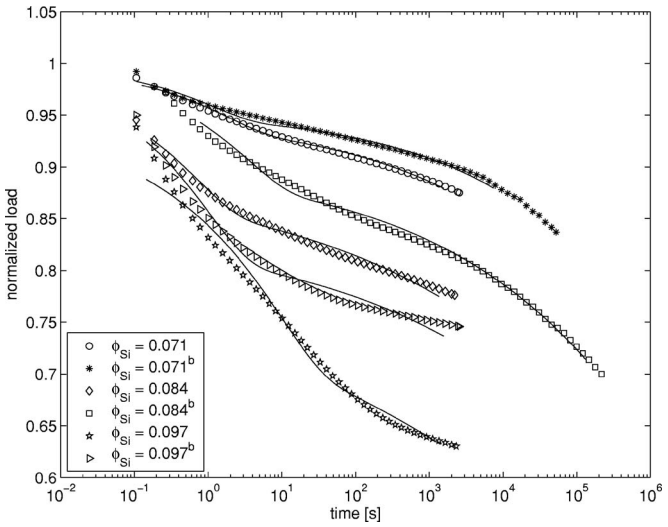

FIG. 5. Normalized load measured in the beam bending experiment on gel treated sandstone samples (series A, acid-catalyzed gel). The estimated silica fraction of the gels is given in the legend. The superscript *b* is used to indicate the duplicate samples prepared with the same gelling solutions as the complementary samples. The solid curves represent the fits using the combined hydrodynamic and VE relaxation function.

Compared to the moduli of the untreated rock samples the moduli are at least as high and in some cases almost 50% higher with respect to the dry rock sample. However, the treated rock samples contain a gelled solution. Though the presence of a liquid, especially water, would soften the rock, the relatively high moduli, extracted from the initial load values, indicate that the gel reinforces the structure. The high degree of VE relaxation observed in most of the relaxation curves is attributed to inelastic behavior of the combined sandstone-gel system upon deflection. The apparent correlation between increasing silica fraction ϕ_{Si} and the overall magnitude of relaxation may be explained by two mechanisms.

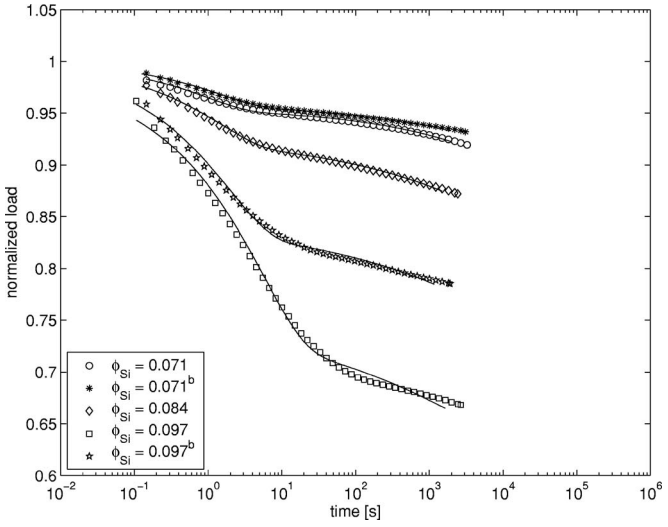

FIG. 6. Normalized load measured in the beam bending experiment on gel treated sandstone samples (series B, base-catalyzed gel). The estimated silica fraction of the gels is given in the legend. The superscript *b* is used to indicate the duplicate samples prepared with the same gelling solutions as the complementary samples. The solid curves represent the fits using the combined hydrodynamic and VE relaxation function.

First of all, the correlation suggests that the reinforcement effect of the gel becomes weaker with increasing ϕ_{Si}. Presumably, the gel is more susceptible to syneresis and loss of adhesion during bending of the sample when ϕ_{Si} is high.[4] The effective modulus would decrease rapidly and result in an apparent strong VE behavior. Second, there could be a thin layer of gel on the upper surface of the sample, lying between the pushrod and the rock, that is crushed during bending, leading to a decrease in deflection of the sample and relaxation of the load. In case the gel layer is weak and compliant with respect to the rock, then the preloading method applied in the experiments should prevent this problem. The high loads obtained in the experiments also suggest that the load is not borne by a weak gel layer. However, if the layer is dense and has a modulus similar to the rock, the pushrod would still effectively bend the rock and produce the high loads. Since the gel layer is thin, it would not directly contribute to the total stress, hence load, in terms of the elastic and hydrodynamic effects. Still, the fast relaxation of the load may be due to a fast deformation of the gel layer in contact with the pushrod and the supports, resulting in a decreasing strain in the rock sample. The effect of this apparent slip mechanism or real slip at the surface is analyzed theoretically in the Appendix.

In the ideal situation the gel would completely fill the pore space of the rock. The overall permeability of the rock would be equal to or smaller than the intrinsic permeability of the gel. To a first-order approximation the permeability would equal the intrinsic permeability of the gel times the porosity (about 0.2) of the rock. Ideally, upon bending the hydrodynamic relaxation would be described by Eq. (4) with an A value of about 0.04. Given the intrinsic permeability of the gels, the corresponding relaxation time τ_R would be about 1×10^4 s for the rock samples treated with acid-catalyzed gel (series A) and τ_R would be about 1×10^3 s for the rock samples treated with base-catalyzed gel (series B). The inflection point, demarcating the final plateau of R, is found at $t\approx0.2\tau_R$.

The relaxation data of the rock samples in series B (see Fig. 6) show a clear inflection point between 10 and 100 s. Despite the high degree of relaxation at the inflection points for the samples with $\phi_{Si}=0.084$ or $\phi_{Si}=0.097$, the relaxation curves were successfully fitted with the common expressions for hydrodynamic and VE relaxation [Eqs. (4) and (10)], which is demonstrated in Fig. 6. The extracted parameters D and A are given in Table III. For the two samples with $\phi_{Si}=0.071$ the amount of hydrodynamic relaxation A corresponds well with the estimated value of 0.04. The extracted permeability varies between 14 and 94 nm^2 without a clear correlation to the estimated silica concentration of the gel inside the rock samples. The estimated silica concentration is based on the initial TMOS concentration as it was for the gel rods, but not corrected for shrinkage. The TMOS concentrations were similar for the gels rods as for the treated rock samples. The overall permeability of the rock samples treated with base-catalyzed gel appears to be at least equal or slightly higher than the intrinsic permeability of the corresponding gel rods. Therefore, the gel does not completely fill all of the pores.

Also, the relaxation data of the rock samples in series A were fitted with the expressions for hydrodynamic and VE relaxation. Again, for the two samples with $\phi_{Si}=0.071$, the curve fit was adequate yielding values for A of about 0.05, and a permeability of 59 ± 7 nm^2 and 95 ± 13 nm^2, respectively. For the higher concentration samples the fit of the relaxation curves was less accurate. As can be observed in Fig. 5, the inflection points in the fitted curves do not agree well with the inflection points in the measured load curves. The extracted permeability for these samples ranges between 8 and 112 nm^2, but these values can only indicate the order of magnitude. Compared to the intrinsic permeability of the acid-catalyzed gel rods, the overall permeability of the rock samples is higher. However, at a given TMOS concentration, the gel rods exhibited a high degree of contraction and pore size reduction. The order of magnitude of the permeability found in series B is comparable to the values found in series A.

V. CONCLUSION

The intrinsic permeability and elastic modulus of various TMOS-based silica alcogels were successfully measured with the method of beam bending. Addition of sodium-chloride, up to 80 mM, and the *p*H of the solution had no significant effect on the modulus, whereas increasing curing and aging times resulted in increased moduli. The permeabilities decreased with increasing silica fraction and aging time. The permeability of the acid-catalyzed gels was on the order of 1 nm^2. The base-catalyzed gels yielded permeabilities 10–100 times higher in magnitude than the acid-catalyzed gels, which is not exclusively attributed to the lower silica fractions of the acid-catalyzed gels, but also to the difference in pore structure of the network. Untreated Bentheim sandstone exhibits a significant VE behavior upon bending, which is due to slip between the grains and due to the low amount of siliceous cement. The permeability of rock samples treated with base-catalyzed gel is on the order of $10-100$ nm^2 without a clear correlation to the silica density of the gel, and is at least as high as the intrinsic permeability of the corresponding gel samples. The permeability of the rock samples treated with acid-catalyzed gel was determined less accurately, but is on the same order of magnitude as for the alkaline series. The findings imply that the gel is not uniformly distributed in the pore space, and that the effectiveness of the treatment varies between the samples, but is insensitive to the *p*H and concentration of the gelling solution. Compared to the untreated sandstone, the overall permeability is reduced by a factor of at least 10^4, so that the gel adequately blocks the pores.

ACKNOWLEDGMENTS

H.J.C. thanks the Netherlands Organisation for Scientific Research (NWO) for their support. The research was further supported by the Dutch Technology Foundation (STW) through project DAR 5756 and additional support was provided by Shell, INA Naftaplin, Chevron, Statoil, ConocoPhilips, and Gaz de France. We thank Timothy Wangler for performing the dilatometry and XRD measurements, and Jane Woodruff for technical assistance with the SEM-EDX.

APPENDIX: EFFECT OF SLIP ON BENDING EXPERIMENTAL

In this appendix we analyze the effect of slip on the measured load W in a three-point beam bending experiment. The effect of slip is modeled in the form of a time-dependent deflection term, i.e., $\Delta=\Delta(t)$. The strain ε_z is directly proportional to the deflection, therefore $\varepsilon_z=\varepsilon_z(t)$. In the following we consider a rectangular elastic plate (as described in the Introduction). The plate is saturated with a Newtonian fluid. The constitutive equations are[15]

$$\varepsilon_x=\frac{1}{E_p}[\sigma_x-\nu_p(\sigma_y+\sigma_z)]-\frac{\hat{b}}{3K_p}P, \tag{A1}$$

$$\varepsilon_y=\frac{1}{E_p}[\sigma_y-\nu_p(\sigma_x+\sigma_z)]-\frac{\hat{b}}{3K_p}P, \tag{A2}$$

$$\varepsilon_z=\frac{1}{E_p}[\sigma_z-\nu_p(\sigma_x+\sigma_y)]-\frac{\hat{b}}{3K_p}P, \tag{A3}$$

where σ is the pore stress, P is the stress in the fluid, which is equal to the pressure but opposite in sign, and $\hat{b}$ is the Biot coefficient defined by

$$\hat{b}=1-\frac{K_p}{K_S}. \tag{A4}$$

After the beam is bent, the pressure in the pore fluid is dissipated due to flow of the fluid within the pores. The continuity equation is given by[15]

$$\frac{\partial P}{\partial\theta}=\frac{\partial^2 P}{\partial v^2}+\kappa\frac{\partial^2 P}{\partial w^2}+\frac{E_p\hat{b}}{3\mu}\frac{\partial\varepsilon_z}{\partial\theta}, \tag{A5}$$

where μ reads

$$\mu=\frac{(1-\rho)K_p}{K_L}+\frac{(\rho-K_p/K_S)K_p}{K_S}+\frac{2(1+\nu_p)}{3}\left(1-\frac{K_p}{K_S}\right)^2. \tag{A6}$$

The solution of Eq. (A5) with the usual boundary conditions ($P=0$ at the boundary) is given by[15]

$$P(v,w,\theta)=\frac{8E_p\hat{b}az}{\mu L^3}\int_0^\theta \Omega_A(\theta-\theta')\Omega_B[\kappa(\theta-\theta')]\frac{d\Delta}{d\theta'}\mathrm{d}\theta', \tag{A7}$$

where

$$\Omega_A(\theta)=-2\sum_{m=1}^{\infty}\frac{(-1)^m}{a_m}\sin(a_m v)\exp(-a_m^2\theta), \tag{A8}$$

$$\Omega_B(\theta)=2\sum_{n=1}^{\infty}\frac{(-1)^n}{b_n}\cos(b_n w)\exp(-\kappa b_n^2\theta), \tag{A9}$$

and $a_m=m\pi$, $b_n=(2n-1)\pi/2$. The load required to sustain the deflection follows from integration of the total stress:

$$W(t) = -\frac{2a^2b}{z}\int_{-1}^{1}\int_{-1}^{1} E_p\left(\frac{\hat{b}}{3K_p}P + \varepsilon_z\right)v\,dv\,dw, \tag{A10}$$

where the strain is given by

$$\varepsilon_z = -\frac{24azv}{L^3}\Delta. \tag{A11}$$

Working out the integrals in Eq. (A10) yields

$$W(\theta) = c_1\Delta(\theta) + c_2\sum_{m=1}^{\infty}\sum_{n=1}^{\infty}\frac{1}{a_m^2 b_n^2}\exp[-\theta(a_m^2+\kappa b_n^2)] \times\int_0^{\theta}\exp[\theta'(a_m^2+\kappa b_n^2)]\frac{d\Delta}{d\theta'}d\theta', \tag{A12}$$

where

$$c_1 = \frac{192a^3bE_p}{3L^3}, \tag{A13}$$

$$c_2 = \frac{256a^3bE_p^2\hat{b}^2}{3\mu L^3K_p}. \tag{A14}$$

An analytical solution is obtained when the deflection follows an exponential decay, for example,

$$\Delta = \Delta_0 H(\theta)\left[(1-h) + h\exp\left(-\frac{\theta\tau_R}{\tau_S}\right)\right], \tag{A15}$$

where H is the Heaviside step function, h reflects the amount of slip ($0\le h\le 1$, and $h=0$ implies no slip), and τ_S is a decay rate. Substituting Eq. (A15) in Eq. (A12) yields

$$W(\theta) = c_1\Delta(\theta) + c_2\sum_{m=1}^{\infty}\sum_{n=1}^{\infty}\frac{\Delta_0}{a_m^2b_n^2}\left\{\exp(-\theta\Gamma_{nm}) + \frac{h\tau_R}{\tau_R-\tau_S\Gamma_{nm}}\left(\exp\left[-\theta\left(\frac{\tau_R}{\tau_S}-\Gamma_{nm}\right)\right] - \exp[-\theta\Gamma_{nm}]\right)\right\}, \tag{A16}$$

where $\Gamma_{nm}=a_m^2+\kappa b_n^2$.

It can be shown that Eq. (A16) reduces to the usual hydrodynamic relaxation expression when $h=0$. In case of a slip, i.e., $h>0$, the decreasing deflection results in an inflection in the load curve similar to that of the hydrodynamic contribution. Some model calculations were performed for an elastic porous plate filled with glycerol and having a permeability of 10 nm^2 and an elastic modulus of 10 GPa. The resulting curves are shown in Fig. 7. The amount of hydrodynamic relaxation A is equal to 0.042 and $h=A$. We note that the relaxation data for the gel-filled rock samples imply that h is larger (up to 0.3) in some cases. The relaxation time τ_R equals 159 s. When $\tau_S \gg \tau_R$ the second inflection due to slipping is well separated from the primary inflection. In the case $\tau_S \ll \tau_R$ the primary inflection in the load curve is brought about by the effect of slip and the second inflection is due to hydrodynamic relaxation. When $\tau_S \approx 0.1\tau_R$ the effects cannot be distinguished, nevertheless, the time at which the inflection is found is still close to $0.2\tau_R$.

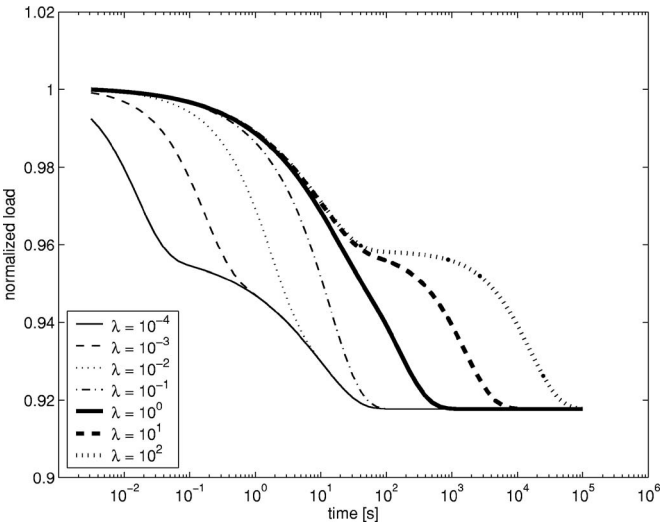

FIG. 7. Calculated load curves for an elastic porous plate, with a permeability of 10 nm^2, an elastic modulus of 10 GPa, and filled with glycerol. The hydrodynamic relaxation time τ_R is equal to 159 s and $A=0.042$. The deflection decays exponentially (see the Appendix) with a relaxation time τ_S equal to $\lambda\tau_R$ and $h=A$. The ratio λ was varied and is indicated in the legend.

[1] P. L. J. Zitha, C. W. Botermans, J. V. D. Hoek, and F. J. Vermolen, J. Appl. Phys. **92**, 1143 (2002).
[2] S. Vossoughi and J. Pet, Sci. Eng. **26**, 199 (2000).
[3] M. I. M. Darwish, R. K. Rowe, J. R. C. van der Maarel, L. Pel, H. Huinink, and P. L. J. Zitha, Can. Geotech. J. **41**, 106 (2004).
[4] C. J. Brinker and G. W. Scherer, *Sol-Gel Science: The Physics and Chemistry of Sol-Gel Processing* (Academic Press Inc., New York, 1990).
[5] R. K. Iler, *The Chemistry of Silica* (John Wiley & Sons, New York, 1979).
[6] H. J. Castelijns, H. P. Huinink, L. Pel, and P. L. J. Zitha, J. Appl. Phys. **100**, 024916 (2006).
[7] G. W. Scherer, J. Non-Cryst. Solids **142**, 18 (1992).
[8] G. W. Scherer, J. Am. Ceram. Soc. **83**, 2231 (2000); **87**, 1612 (2004) (Erratum).
[9] W. Vichit-Vadakan and G. W. Scherer, J. Am. Ceram. Soc. **83**, 2240 (2000); **87**, 1614 (2004) (Erratum).
[10] W. Vichit-Vadakan and G. W. Scherer, J. Am. Ceram. Soc. **85**, 1537 (2002); **87**, 1615 (2004) (Erratum).
[11] M. L. Batzle, D.-H. Han, and R. Hofmann, Geophysics **71**, N1 (2006).
[12] T. L. Chelidze, H. A. Spetzler, and G. A. Sobolev, Pure Appl. Geophys. **147**, 25 (1996).
[13] R. L. Mann and I. Fatt, Geophysics **25**, 433 (1960).
[14] W. Vichit-Vadakan and G. W. Scherer, Cement Concr. Res. **33**, 1925 (2003).
[15] G. W. Scherer, J. Am. Ceram. Soc. **87**, 1517 (2004).
[16] J. Valenza and G. W. Scherer, J. Am. Ceram. Soc. **87**, 1927 (2004).
[17] G. W. Scherer, J. Sol-Gel Sci. Technol. **1**, 169 (1994).
[18] G. W. Scherer, Faraday Discuss. **101**, 225 (1995).
[19] H. Hdach, J. Woignier, J. Phalippou, and G. W. Scherer, J. Non-Cryst. Solids **121**, 202 (1990).
[20] G. W. Scherer, S. A. Pardenek, and R. M. Swiatek, J. Non-Cryst. Solids **107**, 14 (1988).
[21] D. R. Lide, *Handbook Of Chemistry and Physics* (CRC, Boca Raton, FL, 2003).
[22] J. E. Martin and J. Odinek, J. Colloid Interface Sci. **154**, 461 (1992).
[23] G. W. Scherer and R. M. Swiatek, J. Non-Cryst. Solids **113**, 119 (1989).
[24] I. Jiménez González and G. W. Scherer, Environ. Geol. **46**, 364 (2004).
[25] A. N. Tutuncu and M. M. Sharma, Geophysics **57**, 1571 (1992).
[26] M. L. Sheely, Ind. Eng. Chem. Res. **24**, 1060 (1932).
[27] A. N. Tutuncu, A. L. Podio, A. Gregory, and M. M. Sharma, Geophysics **63**, 184 (1998).